EXPERIMENTAL STUDY

Detection of the MicroRNA expression profile in skeletal muscles of burn trauma at the early stage in rats

Zhang Haijun, M.D.,* Yu Yonghui, M.D.,* Chai Jiake, M.D., Duan Hongjie, M.D.

Department of Burn and Plastic Surgery, First Hospital Affiliated to General Hospital of Pla, Beijing, China

ABSTRACT

BACKGROUND: Severe burn injuries are associated with a persistent hypermetabolic response, which causes long-term loss of muscle mass that results in a clinical negative balance of nitrogen and muscle wasting. MicroRNAs (miRNAs) play a critical role in post-transcriptional regulation of gene expression, which negatively regulates gene expression by promoting degradation of target mRNAs or inhibiting their translation. However, the mechanisms of skeletal muscle wasting after severe burn involved in miRNAs still remain unclear.

METHODS: In this study, the alterations of miRNAs expression profile in skeletal muscles of thermal rats were detected at an early stage by microarray. All data were presented as mean±SD. Statistical analysis was determined by independent Student's t-test and one-way ANOVA. The significance was all set at $p<0.05$, and fold change cut-off was 2.0 for microarray. Significant differentially expressed miRNAs were identified through Volcano Plot filtering. Hierarchical clustering was performed using MEV software (v4.6, TIGR).

RESULTS: Thousands of miRNAs could be examined in normal and injured tissues, but only 69 of these were significantly upregulated or down-regulated, which could be used to discriminate skeletal muscles of thermal rats from matched tissues.

CONCLUSION: The deregulated miRNAs probably play a potential role in the pathogenesis of skeletal muscle wasting in burn trauma.

Key words: Burn; microRNA; muscle wasting; profile.

INTRODUCTION

Critical illnesses induce muscle wasting and muscle weakness.[1] Severe burn injuries are associated with a persistent hypermetabolic response, which causes long-term loss of muscle mass that results in a clinical negative balance of nitrogen and muscle wasting. Cutaneous burn and hind limb unloading have an additive effect on muscle atrophy, characterized by loss of muscle mass and decrease in muscle strength in both fast (PL) and slow (SL) twitch muscles.[2–5] Body weight, muscle wet weight and protein weight of rats in burn group were decreased significantly compared with sham group.[6] Following a large burn, skeletal muscle plays an important role in metabolic regulation, such as the synthesis of acute phase proteins and the deposition of new skin.[7]

Growing evidence suggests that the main mechanisms underlying skeletal muscle wasting induced by severe burn include activation of ubiquitin-proteasome pathway,[8–10] myonuclear apoptosis,[1] mitochondrial dysfunction,[5,7] autophagy[1] signaling pathways driving muscle inflammation, and protein metabolism.[11]

MicroRNAs (miRNAs) belong to a group of noncoding small RNAs with a length of 20–24 ribonucleotides, which play a critical role in post-transcriptional regulation of gene expression. Most of them specifically recognize the 3'-untranslated regions (UTR) of their target mRNAs, thereby blocking the process of protein translation or causing mRNA degradation.[12,13] MiRNAs negatively regulate gene expression by promoting degradation of target mRNAs or inhibiting their translation.[14]

The role of miRNAs have been confirmed for a range of common diseases connected to impaired balance of cell proliferation, differentiation and programmed death.[15] It is reported that miRNAs have been shown to play crucial roles in muscle development and in regulation of muscle cell proliferation and

Haijun Zhang and Yonghui Yu contribute equally to this work.

Address for correspondence: Chai Jiake, M.D.
51 Fucheng Road Beijing - China
Tel: +86-10-6686-7972 E-mail: cjk304@126.com

Qucik Response Code

Ulus Travma Acil Cerrahi Derg
2015;21(4):241–247
doi: 10.5505/tjtes.2015.80707

differentiation.[16] Growing evidence indicates that microRNAs significantly impact muscle growth, regeneration and metabolism. MicroRNAs have a great potential to become diagnostic and/or prognostic markers, therapeutic agents and therapeutic targets.[17]

Recently, some research suggests that miRNAs are involved and play an important role in the pathogenesis of CKD and TWEAK induced muscle wasting.[18–21] However, the mechanisms of skeletal muscle wasting after severe burn involved in miRNAs still remain unclear. In this study, microarray analysis was used to detect the alterations of miRNAs expression profile in skeletal muscles of thermal rats at the early stage. Further bio-informatic analysis of deregulated miRNAs will be needed to determine whether these miRNAs play a potential role in the pathogenesis of skeletal muscle wasting in burn trauma.

MATERIALS AND METHODS

This study was approved by the Committee of Science and Technology of the First Hospital affiliated to the General Hospital of PLA (Beijing, China), in accordance with the protocol outlined in the Guide for the Care and Use of Laboratory Animals published by the US National Institutes of Health (NIH publication no. 85–23, revised 1996).

Eight adult male Wistar rats weighing 200 to 220 g were purchased from Chinese Medical Scientific Institute (Beijing, China). A full thickness thermal injury of 30% TBSA was inflicted on the animals by immersing the back of the trunk in 94°C water for 12 s. A weight- and time-matched sham-burn group (n=4) was treated in the same way as the thermal (T) group (n=4), except that the contrast (C) group were immersed in room temperature water. After water immersion, all rats were immediately dried, administered fluid (40 ml/kg of Ringer's lactate solution calculated by the Parkland formula) during the post-burn period, and housed in individual cages with free access to food and water.[22] The animals were euthanized on the third day after thermal injury or sham, and their tibialis anterior (TA) muscles were harvested and stored at -80°C for RNA extraction.

MicroRNA Microarray

MicroRNA arrays of Exiqon feature Tm-normalized LNA™-enhanced capture probes, designed for excellent specificity and sensitivity even for AT-rich microRNAs. In addition, they offer great reproducibility with 99% correlation between arrays and a dynamic range greater than 5 orders of magnitude. The 7th generation of miRCURYTM LNA Array (v.18.0) (Exiqon) contains 3100 capture probes, covering all human, mouse and rat microRNAs annotated in miRBase 18.0, as well as all viral microRNAs related to these species. In addition, this array contains capture probes for 25 miRPlus™ human microRNAs.

RNA Extraction

Total RNA was isolated using TRIzol (Invitrogen) and miRNeasy mini kit (QIAGEN) according to manufacturer's instructions, which efficiently recovered all RNA species, including miRNAs. RNA quality and quantity was measured by using nanodrop spectrophotometer (ND–1000, Nanodrop Technologies) and RNA Integrity was determined by gel electrophoresis.

RNA Labeling

After RNA isolation from the samples, the miRCURY™ Hy3™/Hy5™ Power labeling kit (Exiqon, Vedbaek, Denmark) was used according to the manufacturer's guideline for miRNA labelling. One microgram of each sample was 3'-end-labeled with Hy3TM fluorescent label, using T4 RNA ligase by the following procedure: RNA in 2.0 µL of water was combined with 1.0 µL of CIP buffer and CIP (Exiqon). The mixture was incubated for 30 min at 37°C, and was terminated by incubation for 5 min at 95°C. Then 3.0 µL of labeling buffer, 1.5 µL of fluorescent label (Hy3TM), 2.0 µL of DMSO, 2.0 µL of labeling enzyme were added into the mixture. The labeling reaction was incubated for 1 h at 16°C, and terminated by incubation for 15 min at 65°C.

Array Hybridization

After stopping the labeling procedure, the Hy3TM-labeled samples were hybridized on the miRCURYTM LNA Array (v.18.0) (Exiqon) according to array manual. The total 25 µL mixture from Hy3TM-labeled samples with 25 µL hybridization buffer were first denatured for 2 min at 95°C, incubated on ice for 2 min and then hybridized to the microarray for 16–20 h at 56°C in a 12-Bay Hybridization Systems (Hybridization System - Nimblegen Systems, Inc., Madison, WI, USA), which provides an active mixing action and constant incubation temperature to improve hybridization uniformity and enhance signal. Following hybridization, the slides were achieved, washed several times using Wash buffer kit (Exiqon), and finally dried by centrifugation for 5 min at 400 rpm. Then the slides were scanned using the Axon GenePix 4000B microarray scanner (Axon Instruments, Foster City, CA).

Data Analysis

Scanned images were then imported into GenePix Pro 6.0 software (Axon) for grid alignment and data extraction. Replicated miRNAs were averaged and miRNAs that intensities >=30 in all samples were chosen for calculating normalization factor. Expressed data were normalized using the Median normalization. After normalization, significant differentials expressed miRNAs were identified through Volcano Plot filtering. Hierarchical clustering was performed using MEV software (v4.6, TIGR).

Statistical Analysis

All data were presented as mean±SD. Statistical analysis was

RNA QC EUK

1. RNA Quantification and Quality Assurance by NanoDrop ND-1000

Sample ID	OD260/280 Ratio	OD260/230 Ratio	Conc. (ng/μl)	Volume (μl)	Quantity (ng)	QC result Pass or Fail
1	2.00	2.30	722.96	20	14459.20	pass
4	2.00	2.31	859.83	30	25794.90	pass
5	1.91	2.38	447.36	30	13420.80	pass
6	2.02	2.28	639.62	30	19188.60	pass
37	2.02	2.24	742.03	20	14840.60	pass
39	2.03	2.21	661.48	30	19844.40	pass
41	1.98	2.41	292.58	30	8777.40	pass
41	2.02	2.21	608.70	30	18261.00	pass

• For spectrophotometer, the O.D. A260/A280 ratio should be close to 2.0 for pure RNA (ratios between 1.8 and 2.1 are avveptable). The O.D. A260/A230 ratio should be more than 1.8.

2. RNA Integrity and gDNA contamination test by Denaturing Agarose Gel Electrophoresis

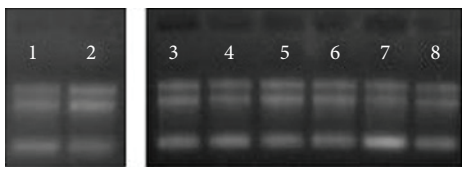

Lane 1: Total RNA of sample 1
Lane 2: Total RNA of sample 4
Lane 3: Total RNA of sample 5
Lane 4: Total RNA of sample 6
Lane 5: Total RNA of sample 37
Lane 6: Total RNA of sample 39
Lane 7: Total RNA of sample 41
Lane 8: Total RNA of sample 42

• The 28S 18S ribosomal RNA bands should be fairly sharp, intens bands. The intensity of the upper band should be about twice that of the lower band. Smaller, more diffuse bands representing low molecular weight RNAs (tRNA and 5S ribosomal RNA) may be present. It is normal to see a diffuse smear of ethidirum bromide staming material migrating between the 18S and 28S ribosomal bands, probably comp rised of mRNA and other heterogeneous RNA species. DNA contamination of the RNA preparation will be evident as a high molecular weight smear or band migrating above the 28S ribosomal RNA band. Degradation of the RNA will be reflected by smearing of ribosomal RNA bands.

Figure 1. Sample RNA quality controlled by Nanodrop 1000 spectrophotometer and denaturing agarose gel electrophoresis.

determined by the independent Student t test and one-way ANOVA. The significance is all set at $p<0.05$, and fold change cut-off is 2.0 for microarray.

RESULTS

Sample RNA Quality Control

Sample quality control data file from Nanodrop 1000 spectrophotometer and standard denaturing agarose gel electrophoresis is performed in Figure 1.

Low Intensity Filtering and Data Normalization

Scanned images were then imported into GenePix Pro 6.0 software (Axon) for grid alignment and data extraction. Replicated miRNAs were averaged and miRNAs that intensities >=30 in all samples were chosen for calculating median normalization factor. Expressed miRNA data were normalized using the median normalization and chosen for differentially expressed miRNAs screening.

Quality Assessment of MiRNA Data after Filtering

The box plots are convenient way to quickly visualize the distribution of a dataset. They are most useful for comparing the distributions of samples. After normalization, the distributions of log2-ratios across every sample are nearly the same.

Correlation Matrix and Scatter Plot

A correlation matrix describes correlation among replicate experiments. The scatter-plot is a visualization that is useful for assessing the variation (or reproducibility) between chips (Fig. 2).

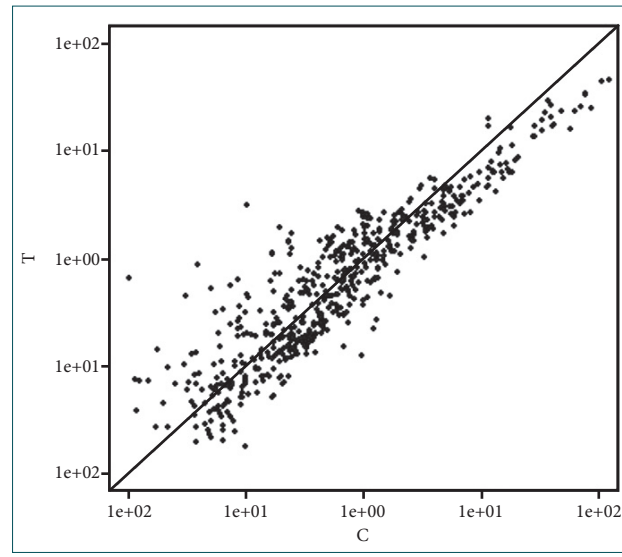

Figure 2. The scatter-plot is for T vs C. The axes of the scatter-plot are the normalized signal values of the samples (Ratio scale).

Differentially Expressed MiRNAs Screening

In order to identify differentially expressed miRNAs with statistical significance, a Volcano Plot filtering (Fig. 3) was performed between the two groups from the experiment. The threshold we used to screen Up or Down regulated miRNAs was Fold Change >=2.0 and p-value <=0.05.

Volcano Plots are useful tools for visualizing differential expression between two different conditions. They are constructed using fold-change values and p-values, and thus, allow you to visualize the relationship between fold-change (magnitude of change) and statistical significance (which takes both magnitude of change and variability into consideration). They also allow subsets of genes to be isolated, based on those values.

Heat Map and Hierarchical Clustering

The heat map diagram shows the result of the two-way hierarchical clustering of miRNAs and samples (Fig. 4). The result of hierarchical clustering shows distinguishable miRNA expression profiling among samples. Each row represents a miRNA and each column represents a sample. The miRNA clustering tree is shown on the left, and the sample clustering tree appears at the top. Cluster analysis arranges samples and miRNAs into groups based on their expression levels, which allows us to hypothesize about the relationships between miRNAs and samples.

Overview of Expression Profiles of MiRNAs

From the miRNA expression profiles, differentially expressed miRNAs were found between samples of skeletal muscles from thermal rats (thermal group) and sham-burn rats (control group). The expression profiles of miRNAs in paired samples were shown by calculating log fold-change Thermal group/Control group (T/C). Agreement was formulated as follows: fold-change cut-off: 2.0. For any fold-change, positive value indicates up-regulation and negative value indicates down-regulation. Log fold-change means log2 value of absolute fold-change. Fold-change and p-values were calculated from the normalized expression.

The miRNAs expression levels were compared between the injured tissues and their matched normal tissues from the microarray data and identified an average of 69 miRNAs that were significantly differentially expressed (2.0-fold) (Table 2). The results demonstrated that thousands of miRNAs could be examined in normal and trauma tissues, but only 4 of these were significantly upregulated and 65 miRNAs were down-regulated, which could be used to discriminate skeletal muscles of thermal rats from matched tissues (Tables 1, 2). Compared to normal tissues, rno-miR–628 (log2 fold-change T/C= 4.518624) was most significantly up-regulated (Table 1), while rno-miR–483–5p (log2 fold-change T/C= 0.129842) was most significantly down-regulated (Table 2). Down-regulated miRNAs were found to be more common than upregulated ones.

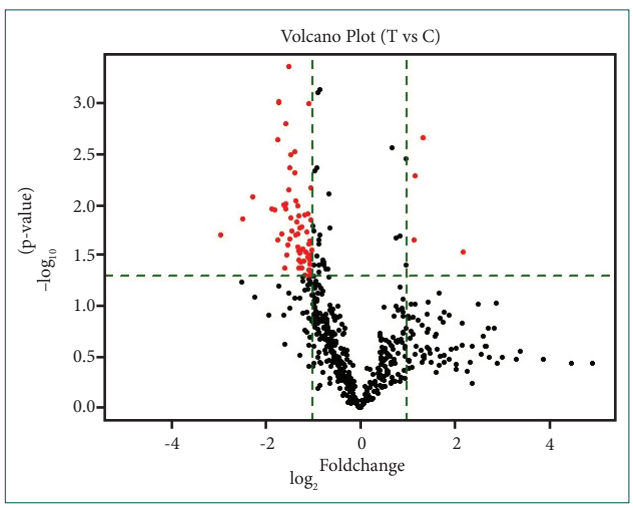

Figure 3. The Volcano Plots is for T vs C. The vertical lines correspond to 2.0-fold up and down, respectively, and the horizontal line represents a p-value of 0.05. So the red point in the plot represents the differentially expressed miRNAs with statistical significance.

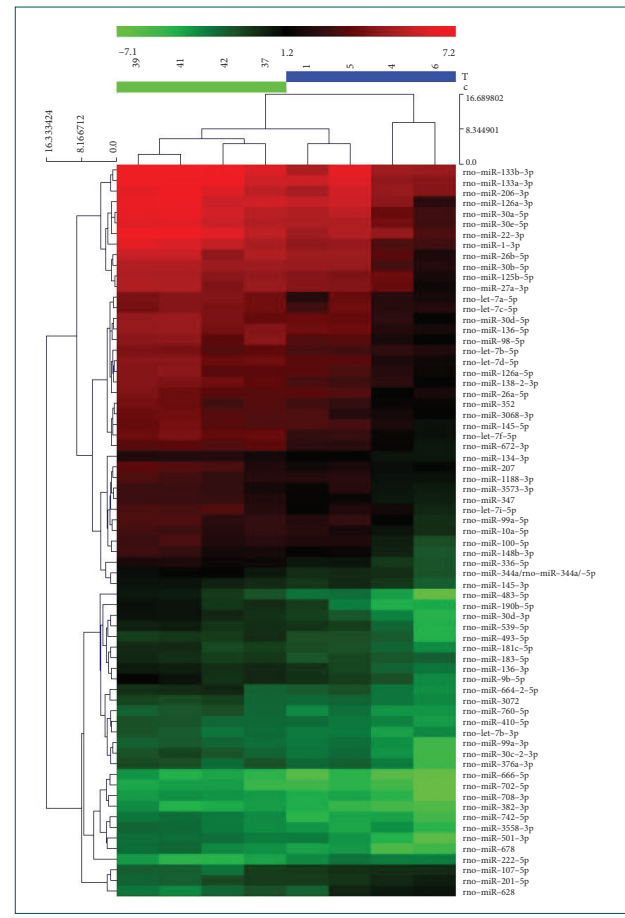

Figure 4. Hierarchical clustering for Differentially Expressed miRNAs (Pass Volcano Plot) in T vs C, those miRNAs that Foreground-Background intensities are smaller than 30 in all samples have been excluded. Red indicates high relative expression, and green indicates low relative expression.

Table 1. Upregulated miRNAs

ID	Name	Fold change	p-value
		T vs C	T vs C
146194	rno-miR–628	4.518624327	0.029565526
147536	rno-miR–107–5p	2.255367446	0.005258001
148133	rno-miR–222–5p	2.538488173	0.002218365
148472	rno-miR–201–5p	2.202553313	0.022298433

• Condition pairs: T vs C.
• Fold Change cut-off: 2.0.
• P-value cut-off: 0.05.
• Column "ID": array ID of the probes, each miRNA always has its unique probe, but some miRNAs may have two different probes.
• Column "Name": the name of each miRNA.
• Column "Fold change": the ratio of normalized intensities between two conditions (use normalized data, ratio scale).
• Column "p-value": T-test result between samples in different groups.

Table 2. Downregulated miRNAs

ID	Name	Fold change	p-value
		T vs C	T vs C
147165	rno-let–7b–5p	0.46888	0.012378
28191	rno-miR–30e–5p	0.371176	0.018072
11208	rno-miR–207	0.329922	0.010157
42686	rno-miR–136–3p	0.390576	0.009291
13485	rno-miR–10a–5p	0.426275	0.016445
42769	rno-let–7b–3p	0.484288	0.031295
148435	rno-miR–672–3p	0.354483	0.000445
30787	rno-miR–125b–5p	0.476592	0.024444
42511	rno-miR–99a–3p	0.480919	0.023114
11273	rno-miR–352	0.40639	0.01948
146086	rno-miR–30a–5p	0.360244	0.021575
169132	rno-miR–382–3p	0.450157	0.049529
46483	rno-miR–27a–3p	0.47107	0.04387
42712	rno-miR–742–5p	0.303099	0.002293
42496	rno-miR–181c–5p	0.435252	0.027404
10943	rno-miR–136–5p	0.417566	0.017105
10977	rno-miR–183–5p	0.489697	0.006857
148131	rno-miR–9b–5p	0.334163	0.041709
46835	rno-miR–483–5p	0.129842	0.019983
14271	rno-miR–539–5p	0.404318	0.026212
146008	rno-miR–26b–5p	0.408252	0.04242
19585	rno-miR–148b–3p	0.346211	0.024874
146144	rno-miR–678	0.301297	0.022062
33596	rno-miR–126a–5p	0.421252	0.036279
42763	rno-miR–347	0.337598	0.001603
31867	rno-miR–145–3p	0.492177	0.027952

Table 2. Downregulated miRNAs (Continue)

ID	Name	Fold change	p-value
		T vs C	T vs C
11182	rno-miR–98–5p	0.337921	0.009954
148187	rno-miR–410–5p	0.478896	0.022755
148417	rno-miR–1188–3p	0.482281	0.034831
148260	rno-miR–664–2–5p	0.342753	0.031127
14303	rno-miR–376a–3p	0.479186	0.04356
11266	rno-miR–336–5p	0.306392	0.001006
19596	rno-miR–30d–5p	0.411276	0.028727
17853	rno-miR–30d–3p	0.210027	0.008348
145968	rno-let–7d–5p	0.40086	0.010225
147592	rno-miR–3072	0.460007	0.018391
148050	rno-miR–3558–3p	0.391432	0.019711
148278	rno-miR–138-2–3p	0.365052	0.003288
148046	rno-miR–344a/ rno-miR–344a–5p	0.386671	0.003028
146137	rno-miR–133a–3p	0.413985	0.029708
147198	rno-miR–26a–5p	0.496159	0.049327
42708	rno-miR–99a–5p	0.483193	0.049396
46626	rno-miR–30c–2–3p	0.338761	0.011011
17347	rno-miR–708–3p	0.486229	0.014214
9938	rno-let–7i–5p	0.353284	0.007104
11020	rno-miR–22–3p	0.287853	0.011369
4610	rno-miR–126a–3p	0.429071	0.042137
11007	rno-miR–206–3p	0.443065	0.036164
145820	rno-let–7c–5p	0.467619	0.012298
148308	rno-miR–702–5p	0.403023	0.025969
148316	rno-miR–134–3p	0.475952	0.001026
17752	rno-let–7f–5p	0.307114	0.000978
146080	rno-miR–666–5p	0.320652	0.019258
146160	rno-miR–133b–3p	0.365804	0.013484
147162	rno-let–7a–5p	0.360995	0.0044
148348	rno-miR–3573–3p	0.456897	0.029535
42641	rno-miR–145–5p	0.483403	0.038325
14294	rno-miR–1–3p	0.273701	0.011079
42472	rno-miR–190b–5p	0.17921	0.013721
145943	rno-miR–100–5p	0.40957	0.034901
168778	rno-miR–501–3p	0.395747	0.01478
146112	rno-miR–30b–5p	0.469834	0.032755
148309	rno-miR–3068–3p	0.412111	0.012813
148059	rno-miR–493–5p	0.444454	0.012715
42741	rno-miR–760–5p	0.385589	0.004902

• Condition pairs: T vs C.
• Fold Change cut-off: 2.0.
• P-value cut-off: 0.05.
• Column "ID": array ID of the probes, each miRNA always has its unique probe, but some miRNAs may have two different probes.
• Column "Name": the name of each miRNA.
• Column "Fold change": the ratio of normalized intensities between two conditions (use normalized data, ratio scale).
• Column "P-value": T-test result between samples in different groups.

DISCUSSION

Burn trauma probably represents the largest stimulus for muscle protein catabolism. This state is characterized by an accelerated catabolism of the lean or skeletal mass that results in a clinical negative balance of nitrogen and muscle wasting.[3] Negative nitrogen balance and accelerated muscle protein breakdown are characteristics of burn injury.[9] Burn survivors experience a profound and prolonged loss of lean body mass, fat mass, and bone mineral density, associated with significant morbidity and reduced quality of life.[23]

MicroRNAs (miRNAs), which regulate the stability and/or the translational efficiency of target messenger RNAs (mRNAs), have been ascribed diverse functions, including regulation of proliferation, differentiation, senescence and death.[14]

Previous studies have showed that miRNAs play critical role in skeletal muscle wasting. In chronic kidney disease (CKD) induced muscle wasting, miR–29 was suppressed in muscle, which leads to higher expression of the transcription factor Ying Yang–1, thereby suppressing myogenesis.[18] FoxO1 is a dominant mediator of CKD-induced muscle wasting, and miR–486 coordinately decreases FoxO1 and PTEN to protect against this catabolic response.[19] Pharmacological agents targeting miR–486 and other miRs, involved in muscle mass regulation, could potentially be developed into therapeutic agents for muscle wasting.[20] TNF-related weak inducer of apoptosis (TWEAK) affects the expression of several genes and microRNAs involved in inflammatory response, fibrosis, extracellular matrix remodeling, and proteolytic degradation which might be responsible for TWEAK-induced skeletal muscle loss. TWEAK inhibits the expression of several miRs including muscle-specific miR–1–1, miR–1–2, miR–133a, miR-133b and miR–206.[21]

In the present study, the result of microarray analysis showed that thermal injury-mediated a total of 69 deregulated miRNAs in the skeletal muscles, in which 4 miRNAs were up-regulated and 65 miRNAs were down-regulated. These deregulated miRNAs may potentially had an important effect in biological pathways essential for skeletal muscle dysfunction to burn trauma.

In addition, since the microarray analysis was just for roughly screening the altered miRNA, we will validate the deregulated miRNAs precisely by the quantitative real-time PCR, predict the target mRNAs of changed miRNAs and perform an deep biomathematics analysis of multiple miRNA target genes by GO and KEGG. This work may be the foundation of further research due to the pathology of muscle dysfunction in burn trauma.

Acknowledgments

This work was supported by the National Natural Science Foundation of China (81120108041, 81471873 and 81201466), State Key Program of the General Logistics Department of PLA (BWS14J048), and Beijing Natural Science Foundation (7144250). The authors wish to thank KangChen Bio-tech Shanghai P.R. China for the microarray work.

Conflict of interest: None declared.

REFERENCES

1. Yasuhara S, Perez ME, Kanakubo E, Yasuhara Y, Shin YS, Kaneki M, et al. Skeletal muscle apoptosis after burns is associated with activation of pro-apoptotic signals. Am J Physiol Endocrinol Metab 2000;279:E1114–21.
2. Wu X, Baer LA, Wolf SE, Wade CE, Walters TJ. The impact of muscle disuse on muscle atrophy in severely burned rats. J Surg Res 2010;164:e243–51. CrossRef
3. Beça A, Egipto P, Carvalho D, Correia F, Oliveira B, Rodrigues A, et al. Nitrogen balance assessment in burn patients. [Article in Portuguese] Acta Med Port 2010;23:883–90. [Abstract]
4. Herndon DN, Ramzy PI, DebRoy MA, Zheng M, Ferrando AA, Chinkes DL, et al. Muscle protein catabolism after severe burn: effects of IGF-1/IGFBP-3 treatment. Ann Surg 1999;229:713–22. CrossRef
5. Padfield KE, Astrakas LG, Zhang Q, Gopalan S, Dai G, Mindrinos MN, et al. Burn injury causes mitochondrial dysfunction in skeletal muscle. Proc Natl Acad Sci U S A 2005;102:5368–73. CrossRef
6. Wu X, Wolf SE, Walters TJ. Muscle contractile properties in severely burned rats. Burns 2010;36:905–11. CrossRef
7. Porter C, Herndon DN, Sidossis LS, Børsheim E. The impact of severe burns on skeletal muscle mitochondrial function. Burns 2013;39:1039–47. CrossRef
8. Solomon V, Madihally S, Yarmush M, Toner M. Insulin suppresses the increased activities of lysosomal cathepsins and ubiquitin conjugation system in burn-injured rats. J Surg Res 2000;93:120–6. CrossRef
9. Chai J, Wu Y, Sheng Z. The relationship between skeletal muscle proteolysis and ubiquitin-proteasome proteolytic pathway in burned rats. Burns 2002;28:527–33. CrossRef
10. Duan X, Berthiaume F, Yarmush D, Yarmush ML. Proteomic analysis of altered protein expression in skeletal muscle of rats in a hypermetabolic state induced by burn sepsis. Biochem J 2006;397:149–58. CrossRef
11. Fang CH, Li B, James JH, Yahya A, Kadeer N, Guo X, et al. GSK-3beta activity is increased in skeletal muscle after burn injury in rats. Am J Physiol Regul Integr Comp Physiol 2007;293:R1545–51. CrossRef
12. Baczyńska D, Michałowska D, Witkiewicz W. The role of microRNA in ischemic diseases-impact on the regulation of inflammatory, apoptosis and angiogenesis processes. [Article in Polish] Przegl Lek 2013;70:135–42. [Abstract]
13. Huang ZP, Neppl RL Jr, Wang DZ. Application of microRNA in cardiac and skeletal muscle disease gene therapy. Methods Mol Biol 2011;709:197–210. CrossRef
14. Luo W, Nie Q, Zhang X. MicroRNAs involved in skeletal muscle differentiation. J Genet Genomics 2013;40:107–16. CrossRef
15. Rogaev EI, Borinskaia SA, Islamgulov DV, Grigorenko AP. Human microRNA in norm and pathology. [Article in Russian] Mol Biol (Mosk) 2008;42:751–64. [Abstract] CrossRef
16. Cardinali B, Castellani L, Fasanaro P, Basso A, Alemà S, Martelli F, et al. Microrna-221 and microrna-222 modulate differentiation and maturation of skeletal muscle cells. PLoS One 2009;4:e7607. CrossRef
17. Wang XH. MicroRNA in myogenesis and muscle atrophy. Curr Opin Clin Nutr Metab Care 2013;16:258–66. CrossRef
18. Wang XH, Hu Z, Klein JD, Zhang L, Fang F, Mitch WE. Decreased miR-29 suppresses myogenesis in CKD. J Am Soc Nephrol 2011;22:2068–76.
19. Xu J, Li R, Workeneh B, Dong Y, Wang X, Hu Z. Transcription factor FoxO1, the dominant mediator of muscle wasting in chronic kidney dis-

ease, is inhibited by microRNA-486. Kidney Int 2012;82:401–11. CrossRef
20. Mak RH, Cheung WW. MicroRNAs: a new therapeutic frontier for muscle wasting in chronic kidney disease. Kidney Int 2012;82:373–4.
21. Panguluri SK, Bhatnagar S, Kumar A, McCarthy JJ, Srivastava AK, Cooper NG, et al. Genomic profiling of messenger RNAs and microRNAs reveals potential mechanisms of TWEAK-induced skeletal muscle wasting in mice. PLoS One 2010;5:e8760. CrossRef
22. Duan H, Chai J, Sheng Z, Yao Y, Yin H, Liang L, et al. Effect of burn injury on apoptosis and expression of apoptosis-related genes/proteins in skeletal muscles of rats. Apoptosis 2009;14:52–65. CrossRef
23. Pedroso FE, Spalding PB, Cheung MC, Yang R, Gutierrez JC, Bonetto A, et al. Inflammation, organomegaly, and muscle wasting despite hyperphagia in a mouse model of burn cachexia. J Cachexia Sarcopenia Muscle 2012;3:199–211. CrossRef

DENEYSEL ÇALIŞMA - *ÖZET*

Sıçanlarda yanık travmalı iskelet kaslarında erken evrede mikro-RNA ekspresyon profili

Dr. Zhang Haijun, Dr. Yu Yonghui, Dr. Chai Jiake, Dr. Duan Hongjie

Yanık ve Plastik Cerrahi Bölümü, Pla Genel Hizmet Hastanesiyle bağlantılı İlk Hastane, Beijing, Çin

AMAÇ: Ciddi yanık travmaları kalıcı hipermetabolik yanıtla ilişkili olup kas kütlesinin uzun süreli kaybına nitrojen ile kas kaybı arasında klinik negatif dengenin bozulmasına yol açmaktradır. MikroRNA'lar (miRNA'lar) hedef mRNA'ların degradasyonunu teşvik ederek veya çevrimlerini engelleyerek gen ekspresyonunu negatif yönde post-transkripisyonel regülasyonunda kritik bir rol oynamaktadır. Ciddi yanık travmasından sonra miRNA'ların katıldığı iskelet kası kaybının mekanizmaları hâlâ anlaşılmış değildir.
GEREÇ VE YÖNTEM: Bu çalışmada mikrodizilim yöntemi kullanılarak erken evrede sıcağa maruz bırakılmış sıçanların iskelet kaslarındaki miRNA'ların ekspresyonlarındaki değişiklikler saptandı. Tüm veriler ortalama±standart sapma olarak sunuldu. İstatistiksel analizlerde bağımsız Student t-testi ve tek-yönlü ANOVA testi kullanıldı. Anlamlılık düzeyi olarak $p<0.05$ ve mikrodizilim yönteminde değişiklik katlarının kestirim değeri olarak 2.0 belirlendi. Ekspresse edilen ve önemli farklılıklar gösteren miRNA'lar Volcano Grafik filreleme yöntemiyle belirlendi. MEV yazılım sistemi (v4.6, TIGR) kullanılarak hiyerarşik küme analizi gerçekleştirildi.
BULGULAR: Normal ve yaralanmış dokularda binlerce miRNA incelenebilmesine karşın bunların yalnızca 69'unda önemli derecede up-regülasyon veya down-regülasyona uğramıştı. Bu yöntem ısıya maruz bırakılmış sıçanların eşleştirilmiş iskelet kası dokularının ayrımında kullanılabilir.
TARTIŞMA: Yanık travmasından sonra iskelet kası kaybının patogenezinde miRNA'ların disregülasyonu potansiyel bir rol oynamaktadır.
Anahtar sözcükler: Kas kaybı; mikroRNA; profil; yanık.

Ulus Travma Acil Cerrahi Derg 2015;21(4):241–247 doi: 10.5505/tjtes.2015.80707